Effects of 1-Butyl-3-methyl Imidazolium Tetrafluoroborate Ionic Liquid on Triton X-100 Aqueous Micelles: Solvent and Rotational Relaxation Studies

ARTICLE *in* THE JOURNAL OF PHYSICAL CHEMISTRY B · JUNE 2011

Impact Factor: 3.3 · DOI: 10.1021/jp111755j · Source: PubMed

6 AUTHORS, INCLUDING:

Chiranjib Ghatak
University of Kansas
38 PUBLICATIONS **570** CITATIONS
SEE PROFILE

Vishal Govind Rao
Bowling Green State University
49 PUBLICATIONS **533** CITATIONS
SEE PROFILE

Sarthak Mandal
Columbia University
44 PUBLICATIONS **444** CITATIONS
SEE PROFILE

Nilmoni Sarkar
IIT Kharagpur
159 PUBLICATIONS **3,689** CITATIONS
SEE PROFILE

THE JOURNAL OF PHYSICAL CHEMISTRY B

ARTICLE

pubs.acs.org/JPCB

Effects of 1-Butyl-3-methyl Imidazolium Tetrafluoroborate Ionic Liquid on Triton X-100 Aqueous Micelles: Solvent and Rotational Relaxation Studies

Rajib Pramanik, Souravi Sarkar, Chiranjib Ghatak, Vishal Govind Rao, Sarthak Mandal, and Nilmoni Sarkar*

Department of Chemistry, Indian Institute of Technology, Kharagpur 721302, WB, India

ABSTRACT: The effect of added room-temperature ionic liquids on the nature of water molecules in the palisade layer of a Triton X-100 (TX-100) micelle has been investigated using solvation and rotational relaxation studies of coumarin 153 in the presence of different wt % of [bmim][BF_4] and thus to understand the changes in micellar palisade layer, especially the entrapped water structures in the palisade layer. It has been observed that in the presence of added [bmim][BF_4] the solvation dynamics becomes faster. It has previously been demonstrated (Behera et al. *J. Chem. Phys.* **2007**, *127*, 184501) that in the present micellar systems, in the presence of [bmim][BF_4] micellar size and aggregation number (N_{agg}) decreases giving rise to more water molecules penetrating in to the micellar phase which results in increased microfluidity. In accordance with solvation dynamics results, fluorescence anisotropy studies also indicate an increased microfluidity for the palisade layer of the TX-100 micelle with the added [bmim][BF_4]. Wobbling-in-cone analysis of the anisotropy data also supports this finding.

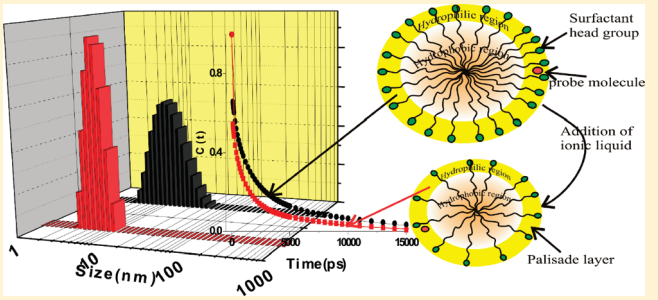

1. INTRODUCTION

Low melting salts that are liquid in ambient conditions are termed room temperature ionic liquids (RTILs). They are usually comprised of organic cations and organic or inorganic anions and are receiving an increasing amount of attention because of their utility as environmentally friendly, green solvents.[1−4] Among the most frequently used RTILs, those based on the substituted imidazolium cations with anions BF_4^-, PF_6^-, and $(CF_3SO_2)_2N^-$ are the most popular ones. RTILs are nonvolatile, thermally stable, nonflammable, and have high conductivity, nonreactivity, wide electrochemical windows, and other properties that make them suitable candidates for multidimensional usage, such as a solvent system for large number of organic and inorganic reaction, catalysis, separation, and electrochemical studies.[5−7] Also, their physicochemical properties can be modulated by changing one of the anions.[8] ILs are not only suitable media for chemical reactions but also promising media for spectroscopic and photophysical studies.[9]

Surfactant solutions comprised of normal or reverse micelles are well studied and are used as media for a variety of chemical reaction and synthesis.[10] Aqueous surfactant solutions have experienced more attention from the research community partly due to the environmentally friendly nature implicit to the aqueous based systems. At ambient conditions, properties of an aqueous solution of a given surfactant depend, among other factors, on the identity of the surfactant. As a result, the physicochemical properties of aqueous surfactant solutions at a given concentration are more or less the same. To modify the physicochemical properties of a given aqueous surfactant solution used an external means, such as changing the temperature or adding various modifiers (e.g., cosolvents, cosufactants, electrolytes, polar organics, nonpolar organics, etc.).[11] Recently to modify the desired physicochemical properties of a surfactant solution environmentally benign substance RTILs are used.[12,13] The effect of RTILs on properties of aqueous surfactant systems is different from that of the common salts. The effectiveness of RTILs in changing the properties of aqueous surfactant systems depends on the kind and extent of interactions of between the ions of RTILs and surfactant headgroup. Since the properties of the RTILs are very much dependent on the constituent ions, various RTILs can be designed using an appropriate combination of the cationic and anionic constituents for some desired properties. Thus utilization of RTILs effectively and favorably to modify properties of dilute aqueous surfactant solutions is attractive both from an environmental and an application point of view. At a lower concentration of RTILs, the electrostatic interaction turned out to be utmost important in determining the physicochemical properties of aqueous surfactant systems. Behera et al[12] has reported that addition of [bmim][BF_4] to aqueous TX-100 results in decreased micellar size, increased critical micellar concentration, and decreased aggregation number N_{agg}. They have also observed that addition of IL to aqueous SB-12 results in decreased N_{agg}; the decrease being significantly more drastic for [bmim][PF_6] addition as compared to that for [bmim][BF_4].

Received: December 10, 2010
Revised: April 26, 2011
Published: May 06, 2011

Scheme 1. Structures of RTIL and C-153

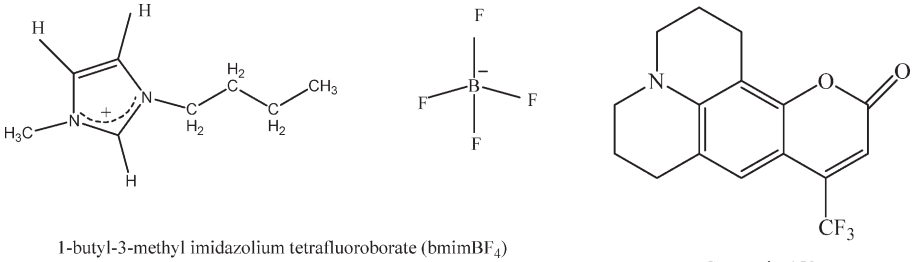

1-butyl-3-methyl imidazolium tetrafluoroborate (bmimBF_4)

Coumarin-153

They have explained the fact on the basis of simple packing considerations, the differences in the size of the two anions.[13a] Recently they have found that addition of IL in SDBS micelle increased the average aggregation suddenly which has been explained on the basis of aromaticity of the IL cation along with the presence of sufficiently aliphatic (butyl or longer) alkyl chains on the IL which appear to be essential for this dramatic critical expansion in self-assembly dimensions within the aqueous SDBS.[13b] They have also studied the effect of IL [hmim][Br] and cosurfactant HeTAB on the modified physicochemical properties of aqueous CTAB, and they found that [hmim][Br] appears to be more severe in altering most of the properties they have investigated.[13c]

Solvent properties in the microenvironment around the reactants in organized media and biological systems can dramatically influence the various chemical reactions such as electron transfer, charge transfer, etc.[14−18] Hence, prior knowledge of the probe environment is very important in understanding, predicting, and controlling various processes in confined media. The study of solvation dynamics in confined media can reveal aspects of the behavior of the water molecules in the probe surroundings and thus can provide details of the microenvironments in the systems.[19−28] It is therefore worthy to study solvation dynamics in micellar media under addition of RTILs to understand the changes in micellar characteristics, such as structure, microviscosity, hydration, etc.

Several groups have investigated the retardation of solvation dynamics in restricted environments. Bhattacharyya et al.[29] studied the solvation dynamics in the Stern layer of the micelles, e.g., neutral (TX-100), cationic (cetyl trimethylammonium bromide, CTAB), and anionic (sodium dodecyl sulfate, SDS), using C-480 and 4-aminophthalimide (4-AP) as a probe. According to a famous phenomenological model of Nandi and Bagchi the slow component of solvation dynamics arises because of an exchange of the water molecules between the bound and the free forms.[30] The existence of the probe in the Stern layer of the micelles is confirmed from steady-state spectroscopic results. Bagchi and co-workers carried out very detailed computer simulations of solvation dynamics of the cesium counterion in micelle. According to them, the slow component of solvation dynamics arises because of hydrogen bonding of the water molecules with the polar head groups (PHG) of the micelle.[31,32] They introduced an energy criterion that a water−PHG hydrogen bond exits if the paired energy between a water molecule and PHG is less than −6.25 kcal mol^{-1}.[31]

In the present work, we have reported the solvent and rotational relaxation studies of aqueous micellar solution of common nonionic surfactant TX-100 upon gradual addition of popular hydrophilic RTIL 1-butyl-3-methylimidazolium tetrafluoroborate ([bmim][BF_4]). The motivation of this work is to understand how the solvent and rotational relaxation in a palisade layer of TX-100 micelle are affected in the presence of added [bmim][BF_4]. We have also used dynamic light scattering (DLS) to investigate structural changes of the micelle. In this work we used Coumarin 153 (C-153) as the solvation probe. The structures of RTIL and C-153 are shown in Scheme1.

2. EXPERIMENTAL SECTION

C-153 (laser grade, Exciton) was used as received. [bmim][BF_4] was obtained from Kanto chemicals (99% purity), and TX-100 was purchased from Aldrich. Doubly distilled deionized water was obtained from a Millipore, Milli-Q academic water purification system having ≥18 MΩ cm resistivity. [bmim][BF_4] and TX-100 were dried in a vacuum oven for 12 h at 70−80 °C before use. A stock solution of 0.2 (M) TX-100 in water was prepared at room temperature (25 °C) by direct weighing. Aqueous TX-100 solutions of the probes were prepared by taking appropriate aliquots of the probes from the stock and evaporating methanol. An aqueous TX-100 solution of desirable concentration was added to achieve the required final probe concentration. Precalculated amount of [bmim][BF_4] was directly added to the aqueous TX-100 solutions.

The absorption and fluorescence spectra were measured using a Shimadzu (model no. UV-2450 Spectrophotometer and a Hitachi F-7000 Spectrofluorimeter. For steady-state experiments, all samples were excited at 408 nm. The detailed time-resolved fluorescence setup is described in our earlier publication.[33] Briefly, the samples were excited at 408 nm using a picosecond laser diode (IBH, Nanoled), and the signals were collected at a magic angle (54.7°) using a Hamamatsu microchannel plate photomultiplier tube (3809U). The instrument response function of our setup was 90 ps. The same setup was used for anisotropy measurements. For the anisotropy decays, we used a motorized polarizer on the emission side. The emission intensities at parallel ($I_{\parallel}$) and perpendicular ($I_{\perp}$) polarizations were collected alternately until a certain peak difference between parallel ($I_{\parallel}$) and perpendicular ($I_{\perp}$) decay was reached. The analysis of the data was done using IBH DAS, version 6, decay analysis software. The same software was also used to analyze the anisotropy data. All the longer and shorter wavelength decays were fitted with biexponential and triexponential functions, respectively, because χ^2 becomes closer to 1, which indicates a good fit. For DLS measurements, we used a Malvern Nano ZS instrument employing a 4mW He−Ne laser (λ = 632.8 nm). All the scattering photons were collected at a 173° scattering angle. The scattering intensity data were processed using the instrumental software to obtain the hydrodynamic diameter (d_h) and size distribution of the sample. The instrument measures the

dx.doi.org/10.1021/jp111755j |J. Phys. Chem. B 2011, 115, 6957–6963

time-dependent fluctuation in the intensity of the light scattered from the particles in solution at a fixed scattering angle. The hydrodynamic diameter (d_h) of the reverse micelle was estimated from the intensity autocorrelation function of the time-dependent fluctuation in intensity. d_h is defined as

$$d_h = \frac{k_b T}{3\pi\eta D} \quad (1)$$

where k_b is the Boltzmann constant, η the viscosity, and D the translational diffusion coefficient. In a typical size distribution graph from the DLS measurement, the *x* axis shows a distribution of size classes in nanometers, while the *y* axis shows the relative intensity of the scattered light. For viscosity measurements we used a Brookfield DV-II+ Pro (Viscometer). The temperature was maintained as a constant by circulating water through the cell holder using a Lab. Companion Thermostat (RG-0525G).

3. RESULTS AND DISCUSSION

3.1. DLS Study. We have measured the hydrodynamic diameter (d_h) of TX-100−water micelles in presence of added [bmim][BF_4]. Figure 1 shows the scattering intensity for the given diameter d_h measured at room temperature of aqueous 0.2 (M) TX-100 in the absence and presence of 15 wt % [bmim][BF_4]. The hydrodynamic diameter (d_h) of TX-100 micelles gradually decreases with addition of [bmim][BF_4] (Table 1). The average hydrodynamic diameter (d_h) of TX-100−water micelles and in presence of 15 wt % [bmim][BF_4] are 10.6 and 5.3 nm, respectively. It is important to mention that our average diameter of aqueous TX-100 micelles and in presence of various wt % [bmim][BF_4] are similar to those reported in literature.[12] They have found another interesting outcome is the micellar size distribution narrows considerably upon addition of [bmim][BF_4] demonstrating that the micellar assemblies are more monodisperse in the presence of RTIL.

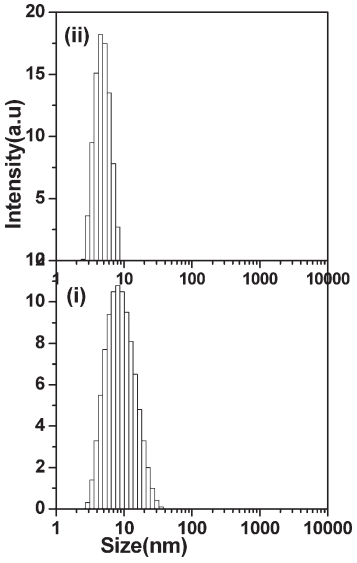

Figure 1. Size distribution in a 0.2 (M) TX-100 water micelle (measured by DLS) (i) in absence of [bmim][BF_4] and (ii) in presence of 15 wt % [bmim][BF_4].

3.2. Steady State Results. In water, the absorption and emission peaks of C-153 are at 432 and 548 nm, respectively. In

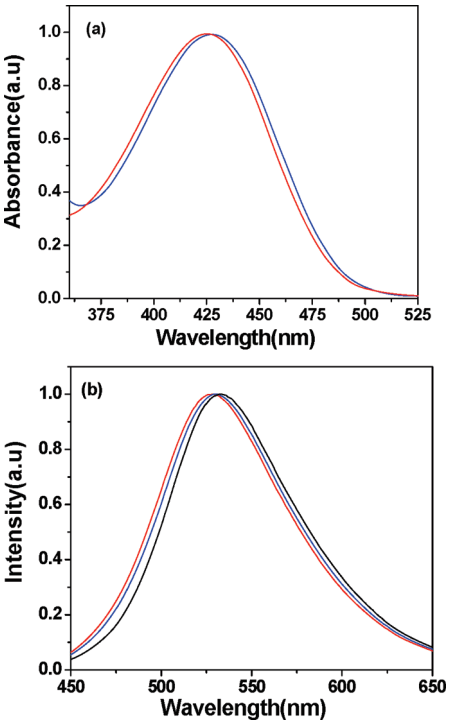

Figure 2. (a) Absorption spectrum of C-153 in 0.2 (M) TX-100 micelle in absence of RTIL (red) and in presence of 15 wt % [bmim][BF_4] (blue), respectively. (b) Emission spectrum of C-153 in 0.2 (M) TX-100 micelle in absence of RTIL (red) and in presence of 5 wt % (blue) and 15 wt % (black) [bmim][BF_4], respectively.

Table 2. Steady State Absorption and Emission Maxima of C-153 in 0.2 (M) TX-100−Water Micelles in the Presence of Various wt % [bmim][BF_4]

systems	$^{abs}\lambda_{max}$ (nm)	$^{em}\lambda_{max}$ (nm)
0.2 (M) TX-100 micelle	426	529
0.2 (M) TX-100 micelle + 5 wt % [bmim][BF_4]	427	530
0.2 (M) TX-100 micelle + 10 wt % [bmim][BF_4]	428	531
0.2 (M) TX-100 Micelle + 15 wt % [bmim][BF_4]	429	533
neat [bmim][BF_4]	422	528
H_2O	432	548

Table 1. Decay Parameters of $C(t)$ of C-153 in 0.2 (M) TX-100−Water Micelle with Various wt % of [bmim][BF_4]

systems	α_1	α_2	α_3	τ_1 (ns)	τ_2 (ns)	τ_3 (ns)	$\langle\tau_{sol}\rangle$ (ns)	size (nm)
0.2 (M) TX-100 micelle	0.33	0.41	0.26	0.047	1.08	7.03	2.29	10.6
0.2 (M) TX-100 micelle + 5 wt % [bmim][BF_4]	0.37	0.39	0.24	0.044	0.99	6.74	2.02	8.5
0.2 (M) TX-100 micelle + 10 wt % [bmim][BF_4]	0.40	0.39	0.21	0.040	0.89	6.67	1.76	6.7
0.2 (M) TX-100 micelle + 15 wt % [bmim][BF_4]	0.43	0.38	0.19	0.038	0.82	5.57	1.39	5.3

dx.doi.org/10.1021/jp111755j |*J. Phys. Chem. B* 2011, 115, 6957–6963

Table 3. Decay Parameters of Rotational Relaxation of C-153 in 0.2 (M) TX-100−Water Micelles with Various wt % of [bmim][BF_4]

systems	α_1	α_2	τ_1 (ns)	τ_2 (ns)	$\langle\tau_{avs}\rangle$ (ns)	R_0	viscosity (cP)
0.2 (M) TX-100 micelle	0.35	0.65	0.61	2.83	2.05	0.34	5.80
0.2 (M) TX-100 micelle + 5 wt % [bmim][BF_4]	0.35	0.65	0.63	2.61	1.92	0.34	3.25
0.2 (M) TX-100 micelle + 10 wt % [bmim][BF_4]	0.35	0.65	0.60	2.40	1.76	0.34	2.95
0.2 (M) TX-100 micelle + 15 wt % [bmim][BF_4]	0.36	0.64	0.45	2.01	1.45	0.33	2.70

TX-100−water micelles at 0.2 (M) both the absorption and emission peak of C-153 exhibit a blue shift (Table 2). In TX-100 micelle absorption and emission peaks of C-153 are at 426 and 529 nm, respectively. The absorption and steady-state fluorescence spectra of C-153 in TX-100 micellar solution were recorded in the presence of added [bmim][BF_4] (Figure 2). It is seen that the spectra of the C-153 dye in TX-100 micelles show slightly red shifts in the presence of [bmim][BF_4]. The change in the size and hydration of the TX-100 micelle presence of [bmim][BF_4] results in an increase the polarity experienced by the probe for the micellar microenvironment. It was inferred that as micellar hydration increases, the probe in the palisade layer undergoes a relative migration toward the micellar surface, causing it to experience a more polar microenvironment for the micelle. From absorption and steady-state fluorescence spectra, it is also seen that the spectral width remains almost unaffected with the added RTIL, suggesting that the distribution of the dye molecules in the palisade layer is not altered significantly by the presence of the RTIL.

3.3. Viscosity Measurement. We have also measured the viscosity of TX-100 micellar solutions in the presence of various amounts of [bmim][BF_4]. We have also measured the bulk viscosity of neat [bmim][BF_4]. With gradual addition of [bmim][BF_4] in TX-100 water micelle the bulk viscosity of the solution gradually decreases. The bulk viscosities of [bmim][BF_4] and in TX-100 water micelle in the presence of [bmim][BF_4] are listed Table 3.

3.4. Time-Resolved Studies. *3.4.1. Time-Resolved Anisotropy Measurements.* Absorption and emission spectra can give a qualitative idea regarding the location of the probe molecules. This can be more accurately predicted by the time-resolved fluorescence anisotropy. Time resolved anisotropy, $r(t)$, is calculated using the following equation

$$r(t) = \frac{I_{\parallel}(t) - GI_{\perp}(t)}{I_{\parallel}(t) + 2GI_{\perp}(t)} \quad (2)$$

where G is the correction factor for detector sensitivity to the polarization direction of emission. $I_{\parallel}(t)$ and $I_{\perp}(t)$ are fluorescence decays polarized parallel and perpendicular to the polarization of the excitation light, respectively. The G factor for our setup is 0.6. To understand the changes in the microviscosity for the palisade layer, we measured fluorescence anisotropy decays for C-153 dye in the TX-100 micellar solution in the presence of different wt % of [bmim][BF_4]. Representative anisotropy decays of C-153 in micelle in the absence and presence of [bmim][BF_4] are shown in Figure 3. In the presence of 15 wt % [bmim][BF_4] within the aqueous TX-100 the bulk viscosity of the medium decreases from 5.8 to 2.7 cP; consequently, the rotational time decreases from 2.05 to 1.39 ns (see Table 3). The decreased rotational relaxation time from 2.05 to 1.39 ns, which is around 30% decreased from the initial value. However Behara et al.[12] reported that steady-state anisotropy value of rhodamine 6G decreases 20% upon addition of 20 wt % [bmim][BF_4] from ~0.2 to 0.16. So the decrement of

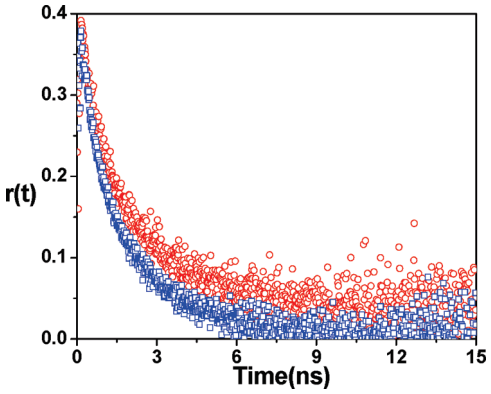

Figure 3. Fluorescence anisotropy decay of C-153 in 0.2 (M) TX-100 water micelle in the absence of [bmim][BF_4] (○) and in the presence of 10 wt % [bmim][BF_4] (□), respectively.

anisotropy value in case of R6G is less than that of the C-153 may be due to the different partitioning of the probes in two pseudophase (R6G has more polar character as compared to C-153). The anisotropy decays in the micelles are found to be biexponential in nature. In micellar solutions, for a probe residing in the palisade layer, different kinds of motions can contribute to the observed fluorescence anisotropy decay.[34−37] The biexponential anisotropy decays in these micelle can be explained with the help of a two-step model and wobbling-in-a-cone model. The two-step model shows that the observed slow rotational relaxation (τ_2) is a convolution of the relaxation time corresponding to the overall rotational motion of the micelles (τ_m) and lateral diffusion of the probe (τ_D). The wobbling-in-a-cone model describes the internal motion of the probe (τ_e) in terms of a cone angle (θ_0) and wobbling diffusion coefficient (D_w). The τ_m, τ_D, τ_e, θ_0, and D_w values are calculated from the relevant equations defined by Quitevis et al.[36] as follows in eqs 3 and 4

$$\frac{1}{\tau_2} = \frac{1}{\tau_D} + \frac{1}{\tau_m} \quad (3)$$

$$\frac{1}{\tau_1} = \frac{1}{\tau_e} + \frac{1}{\tau_2} \quad (4)$$

where τ_1 and τ_2 are the observed fast and slow components. The results are summarized in Table 4. Overall rotation of the micelles can be estimated using the Stokes−Einstein−Debye relationship[36,37]

$$\tau_m = \frac{4\pi\eta r_h^3}{3kT} \quad (5)$$

where η is the viscosity of the water, r_h is the hydrodynamic radius of the micelles, and k and T are Boltzmann's constant and the absolute temperature, respectively. From Table 4, it is inferred that τ_m values are in the range of several nanoseconds. It could be noted that the τ_m values are several orders of magnitude higher than the τ_1 and τ_2

Table 4. Analytical Parameters Obtained from the Anisotropy Decays of C-153 in 0.2 (M) TX-100 Micelles with Various wt % of [bmim][BF_4]

systems	τ_e (ns)	τ_m (ns)[a]	τ_D (ns)	D_w (10^{-8} s^{-1})	Θ_0 (deg)	S
0.2 (M) TX-100 micelle	0.78	199	2.83	172.9	69	0.81
0.2 (M) TX-100 micelle + 5 wt % [bmim][BF_4]	0.78	99	2.70	178.1	69	0.81
0.2 (M) TX-100 micelle + 10 wt % [bmim][BF_4]	0.73	52.5	2.52	190.2	69	0.81
0.2 (M) TX-100 micelle + 15 wt % [bmim][BF_4]	0.58	26	2.17	239.4	68	0.80

[a] τ_m= Overall rotation of the micelle has been estimated using Stokes−Einstein−Debye equation.

values. Therefore, overall rotation does not contribute to the anisotropy decays. Thus, slow components are arising due to the lateral diffusion of the probe. This is because the reorientation time for the overall rotation of the micelle becomes very long and consequently the fluorescence depolarization due to this process becomes negligible. It has been reported that hydrogen bonds exist between the water molecules and the polar head groups (PHG) of the micelle.[31] It is also reported that addition of [bmim][BF_4] in TX-100 micellar solutions decreases the micellar size, aggregation number, and increased water penetration in the palisade layer of the micellar phase.[12] Such a decrease in aggregation number and increased water penetration can reduce the contraction of the polar oxoethylene headgroups which reduces the constraint on motions of the probes in the palisade layer. This effect will be especially prominent in the lateral diffusion of the probe in the micelle. Accordingly, the decrease in slow component of anisotropy decay is expected to be relatively more than that in fast component. We have also calculated the order parameter (S) to get a clear idea about the location of the probe. The value of S is obtained from the relative amplitude of the slow component as $S^2 = a_2$. Inspection of the table 3 reveals that there is a gradual decrease of the time constant of slow component (τ_2). However, there is no variation in the relative amplitude of the slow component (a_2) which is probably due to the inherent limitations associated with the recovery of all the parameters from the anisotropy decays accurately. The magnitude of the S is a measure of spatial restriction and has values from zero (unrestricted motion) to 1 (completely restricted motions). The high value of the order parameter indicates that probe molecules are experiencing restricted motions, which is possible if they are located in the core or palisade layer of the micelle.

We can calculate the cone angle θ_0 and wobbling diffusion coefficient D_W from eq 6 and 7

$$\theta_0 = \cos^{-1}\left[\frac{1}{2}(1+8S)^{1/2} - 1\}\right] \quad (6)$$

$$D_W = \frac{7\theta^2}{24\tau_e} \quad (7)$$

Where θ_0 is cone angle in radians. The D_w value of C-153 increases with increasing added [bmim][BF_4]. Smaller micellar size with significantly lower N_{agg} due to presence of [bmim][BF_4] within the aqueous TX-100 results in more water penetration in to the micellar phase giving rise to increased microfluidity. Hence, the microviscosity around the probe in micellar palisade layer also decreases, and the value of D_w increases. Behara et al.[12] have also measured microfluidity in these systems using steady-state emission of 1, 3 bis-(1-pyrenyl) propane (BPP). According to their results on addition of 10 wt % [bmim][BF_4] the monomer to excimer emission intensity ratio (I_M/I_E) of BPP decreases from 9 to 8 which is around 11% decrease from initial value. The calculated wobbling diffusion coefficient value increases from 172.9 × 10^{-8} s^{-1} to 190.2 × 10^{-8} s^{-1} on addition of 10 wt % [bmim][BF_4], i.e., around 11% increase from initial value. So the same extent of changes may be due to similar partition coefficient of the two hydrophobic probes BPP and C-153 in the micellar systems.

3.4.2. Solvation Dynamics Study. To study solvent relaxation dynamics, we collected the time-resolved decays monitored at different wavelength for all the systems. The decays at the red edge of the emission spectra were preceded by a growth in fraction of nanosecond time scale, whereas decays at the short wavelengths are fast. The wavelength-dependent behavior of temporal decays of C-153 clearly indicates that solvent relaxation is taking place in these systems. The time-resolved emission spectra (TRES) were constructed using the procedure of Fleming and Maroncelli.[38] The TRES at a given time t, $S(\lambda, t)$, is obtained by the fitted decays, $D(t,\lambda)$, by relative normalization to the steady-state spectrum $S_0(\lambda)$, as follows

$$S(\lambda,t) = D(\lambda,t)\frac{S_0(\lambda)}{\int_0^\infty D(\lambda,t)\,dt} \quad (8)$$

Each TRES was fitted by a log-normal line shape function, which is defined as

$$g(\nu) = g_0 \exp\left[-\ln 2\left(\frac{\ln[1+2b(\nu-\nu_p)]/\Delta}{b}\right)^2\right] \quad (9)$$

where g_0, b, νp, and Δ are the peak height, asymmetric parameter, peak frequency, and width parameter, respectively.

We have obtained the peak frequency from the log-normal fitting of TRES. The solvation dynamics was monitored by the solvent response function defined as

$$C(t) = \frac{\nu(t) - \nu(\infty)}{\nu(t=0) - \nu(\infty)} \quad (10)$$

$\nu(t = 0)$ is the frequency at "zero-time", as calculated by the method of Fee and Maroncelli.[39] $\nu(\infty)$ is the frequency at "infinite time", which may be taken as the maximum of the steady-state fluorescence spectrum if solvation is more rapid than the population decay of the probe. $\nu(t)$ is determined by taking the maxima from the log-normal fits as the emission maximum. In most of the cases, however, the spectra are broad, so there is some uncertainty in the exact position of the emission maxima. Therefore, we have considered the range of the raw data points in the neighborhood of the maximum to estimate an error for the maximum obtained from the log-normal fit. Depending on the width of the spectrum (i.e., zero-time, steady-state, or TRES), we have determined the typical uncertainties as follows: zero time ≈ steady state (±120 cm^{-1}) < time-resolved (±200 cm^{-1}) emission. We use these uncertainties to compute error bars for $C(t)$.

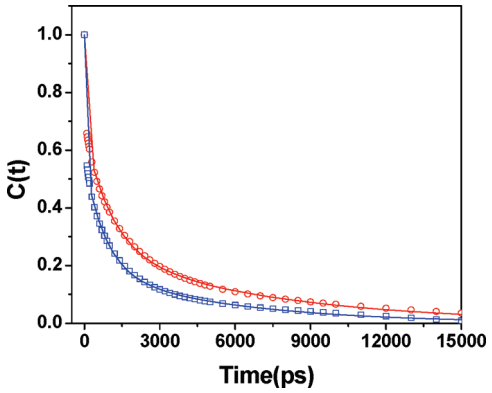

Figure 4. Decay of solvent correlation function of $C(t)$ of C-153 in 0.2 (M) TX-100 water micelle in absence of [bmim][BF_4] (○) and in presence of 15 wt % [bmim][BF_4] (□), respectively.

Finally, in generating $C(t)$, the first point was obtained from the zero time spectrum. The second point was taken at the maximum of the instrument response function, which, having a full width at half-maximum of ≤100 ps, was taken to be 100 ps. The solvent response function $(C(t))$ was fitted to a triexponential decay function

$$C(t) = \alpha_1 \exp^{(-t/\tau_1)} + \alpha_2 \exp^{(-t/\tau_2)} + \alpha_3 \exp^{(-t/\tau_3)} \quad (11)$$

where τ_1, τ_2, and τ_3 are the relaxation times with amplitude α_1, α_2, and α_3, respectively.

In the micellar solution with the probe in the palisade layer, there is a sharp change in the dielectric constant within the molecular dimensions.[40] When explaining the solvent relaxation process in the micelle, it is important to consider the solvent structures around the probe. Accordingly, the molecular approach for the solvent relaxation process, which takes account of the solvent structures around the probe,[39,41] appears to be more logical for understanding the results in micellar solutions, although the situation in the micellar media is much more complex than that in homogeneous solution. Inside the micellar palisade layer, the movement of the water molecules is supposed to be hindered very much. Accordingly, the solvation process is expected to be substantially slower in micellar media than in bulk water.[24,25] Moreover, it is likely that the response from the few water molecules that are adjacent to the probe will be much slower than the collective response of the water molecules that are distance from the probe.[39,41] Thus in micellar media the longer solvation component is determined mainly by the response of the few water molecules that are adjacent to the probe, and the shorter solvation component is determined mainly by the collective response of a relatively large number of water molecules that are somewhat away from the probe.

To comprehend the solvation dynamics results, a thorough understanding of the micelle structure and location of the probe within the micelle is necessary. UV, fluorescence, and anisotropy study showed that the probe molecule resides in the palisade layer of the micelle. DLS experiments show that the hydrodynamic diameter decreases from 10.6 to 5.3 nm in the presence of 15 wt % [bmim][BF_4]. On addition of the IL [bmim][BF_4] to the TX-100 micelle, the solvent relaxation of C-153 is faster (Figure 4 and Table 1). It can be seen in Figure 4 that, in the TX-100 micellar system, faster decays of solvent correlation function $C(t)$ have been observed for at higher weight % of ILs. We observed 2.29 ns average solvation time in TX-100 micelle in the absence of [bmim][BF_4]. The value of the fast component was 1.08 ns, and that of the slow component was 7.03 ns with relative contribution of 41 and 26%, respectively. In the micelle at 15 wt %, that is, with higher RTIL content, we observed 1.39 ns average solvation time, and the value of the fast component was 0.82 ns and that of the slow component were 5.57 ns with relative contribution 38 and 19%, respectively. We also observed a very fast component with time constant around 40 ps, and the relative contributions of the component are 33 and 43% in the absence and presence of 15 wt % [bmim][BF_4], respectively. The decay times of the components are shorter than that of the instrument resolution (90 ps). We have fitted the time zero spectrum using the Fee and Maroncelli[39] method, and thus we can obtain the ultrafast components. The ultrafast components are actually the missing dynamics in the studied systems. The change of fast components remains very small, whereas the slower components became faster. We also observed the relative contribution of the faster component, and the slower components decrease in presence of RTIL. The values of faster components and the slower components became faster, the relative contribution of the faster and the slower components decreases, so we observed a decrease in average solvation time. For example, when we use TX-100 micelle in absence of RTIL, we got the faster component 1.08 ns having relative contribution of 41% and slower component 7.03 ns having relative contribution of 26%. Therefore, the average solvation time varies from 2.29 to 1.39 ns in presence of 15 wt % [bmim][BF_4] (See Table 1). It is inferred that in the presence of [bmim][BF_4] more water molecules penetrate the micellar phase, therefore hydrogen bonding interaction of water to the surfactants ether groups apparently becomes saturated and thus excess water resides freely in the palisade layer. Hence, in presence of [bmim][BF_4] water molecules encounter less restricted environment in the palisade layer of micelle. Therefore, faster solvation dynamics at the higher [bmim][BF_4] concentrations due to less restricted environment of water molecules in palisade layer causes the solvation time to become faster. The present results with [bmim][BF_4] are found to be substantially different than those obtained previous studied by Kumbhakar et al.[27] with salts such as NaCl, KCl, and CsCl. They have found that the ions reside in the palisade layer, and because of the hydration of the ions, especially the cations, the water molecules in the palisade layer undergo a kind of clustering, causing the increase in microviscosity, consequently retardation in solvation dynamics has been observed in the presence of salts.

4. CONCLUSIONS

Solvation dynamics in the TX-100 micellar solution in the presence of [bmim][BF_4] show faster solvation. These results indicate a possible change in the nature of the water molecules present in the palisade layer. Behera et al. have found that in the present micellar systems in the presence of RTIL micellar size and N_{agg} decrease giving more water molecules penetration in to the micellar phases increases the microfluidity. We have also observed these phenomena by using a different technique "dynamics of solvent and rotational relaxation" in these media which more precisely characterizes motion of water molecules in palisade layer of micelle. In the presence of [bmim][BF_4] the water molecule more penetrate further into the micellar phase; therefore hydrogen bonding interaction of water to the

surfactants ether groups apparently becomes saturated and thus excess water resides freely in the palisade layer. Hence in presence of [bmim][BF_4], water molecules encounter less restricted environment in the palisade layer of the micelle. Accordingly, solvation dynamics become faster as [bmim][BF_4] is added to the solution. The measured fluorescence anisotropy results in the present systems also qualitatively support the above inferences drawn from the solvation dynamics studies in the TX-100 micelle in the presence of different [bmim][BF_4] concentrations.

AUTHOR INFORMATION

Corresponding Author

*E-mail: nilmoni@chem.iitkgp.ernet.in. Fax: 91-3222-255303.

ACKNOWLEDGMENT

N.S. is thankful to Department of Science and Technology, Council of Scientific and Industrial Research (CSIR), and the Board of Research in Nuclear Sciences (BRNS), Government of India for generous research grants. R.P, C.G, V.G.R., and S.M are thankful to CSIR for research fellowships. S.S is thankful to BRNS for SRF.

REFERENCES

(1) Seddon, K. R. *Nature* **2003**, *2*, 363.
(2) Anderson, J. L.; Ding, J.; Welton, T.; Armstrong, D. W. *J. Am. Chem. Soc.* **2002**, *124*, 14247.
(3) Anderson, J. L.; Armstrong, D. W.; Wei, G. T. *Anal. Chem.* **2006**, *78*, 2893.
(4) Pandey, S. *Anal. Chim. Acta* **2006**, *556*, 38.
(5) (a) *Ionic Liquids in Synthesis*; Welton, T., Wasserscheid, P., Eds.; VCH-Wiley: Weinheim, Germany, 2002. (b) Dupont, J.; de Suza, R. F.; Suarez, P. A. Z. *Chem. Rev.* **2002**, *102*, 3667. (c) Rantwijk, F.; van; Sheldon, R. A. *Chem. Rev.* **2007**, *107*, 2785. (d) Wasserscheid, P.; Keim, W. *Angew. Chem., Int. Ed.* **2000**, *39*, 3772.(e) Seddon, K. R.; Stark, A.; Torres, M. J. In *Clean Solvents: Alternative Media for Chemical Reactions and Processing*; Abraham, M., Moens, L., Eds.; ACS Symposium Series 819; American Chemical Society: Washington, DC, 2002.
(6) Huddleston, J. G.; Willauer, H. D.; Swatlowski, R. P.; Visser, A. E.; Rodgers, R. D. *Chem. Commun.* **1998**, 1765.
(7) (a) Cadena, C.; Anthony, J. L.; Shah, J. K.; Morrow, T. I.; Brennecke, J. F.; Maginn, E. J. *J. Am. Chem. Soc.* **2004**, *126*, 5300. (b) Dickinson, V. E.; Williams, M. E.; Hendrickson, S. M.; Masui, H.; Murray, R. W. *J. Am. Chem. Soc.* **1999**, *121*, 613.
(8) Patrascu, C.; Gauffre, F.; Nallet, F.; Bordes, R.; Oberdisse, J.; de Lauth-Viguerie, N.; Mingotaud, C. *Chem. Phys. Chem.* **2006**, *7*, 99.
(9) (a) Hu, Z.; Huang, X.; Annapureddy, H. V. R.; Margulis, C. J. *J. Phys. Chem. B* **2008**, *112*, 7837. (b) Santhosh, K.; Samanta, A. *J. Phys. Chem. B* **2010**, *114*, 9195. (c) Kashyap, H. K.; Biswas, R. *J. Phys. Chem. B* **2010**, *114*, 254. (d) Page, T. A.; Kraut, N. D.; Page, P. M.; Baker, G. A.; Bright, F. V. *J. Phys. Chem. B* **2009**, *113*, 12825.
(10) (a) Moroi, Y. *Micelles: Theoretical and Applied Aspects*; Springer: New York, 1992. (b) Jones, M. J.; Chapman, D. *Micelles, Monolayers and Biomembranes*; Wiley-LISS: New York, 1995. (c) Shah, D. O. *Micelles, Microemulsions and Monolayers*; CRC: Boca Raton, 1998. (d) Rosen, M. J. *Surfactants and Interfacial Phenomena*; Wiley: New York, 1978. (e) Fendler, J. H. *Membrane Mimetic Chemistry: Characterizations and Applications of Micelles, Microemulsions, Monolayers, Bilayers, Vesicles and Host-Guest Systems*; Wiley: New York, 1983.
(11) (a) Dutkiewicz, E.; Jakubowska, A. *Colloid Polym. Sci.* **2002**, *280*, 1009. (b) Neves, A. C. S.; Valente, A. J. M.; Burrows, H. D.; Ribeiro, A. C. F.; Lobo, V. M. M. *J. Colloid Interface Sci.* **2007**, *306*, 166. (c) Forland, G. M.; Samseth, J.; Gjerde, M. I.; Hoiland, H.; Jensen, A. O.; Mortensen, K. *J. Colloid Interface Sci.* **1998**, *203*, 328. (d) Dutkiewicz, E.; Jakubowska, A. *J. Phys. Chem. B* **1999**, *103*, 9898. (e) Srinivasan, V.; Blankschtein, D. *ibid.* **2003**, *19*, 9946.
(12) Behera, K.; Pandey, M. D.; Porel, M.; Pandey, S. *J. Chem. Phys.* **2007**, *127*, 184501.
(13) (a) Behera, K.; Pandey, S. *J. Colloid Interface Sci.* **2009**, *331*, 196. (b) Rai., R.; Baker, G. A.; Behera, K.; Mahanty, P.; Kurur, N. D.; Pandey, S. *Langmuir* **2010**, *26*, 17821. (c) Behera, K.; Om, H.; Pandey, S. *J. Phys. Chem. B* **2009**, *113*, 786. (d) Behera, K.; Pandey, S. *Langmuir* **2008**, *24*, 6462. (e) Behera, K.; Dahiya, P.; Pandey, S. *J. Colloid Interface Sci.* **2007**, *307*, 235.
(14) Altschuler, M.; Heddens, D. K.; Diveley, R. R.; Krescheck, G. C. *BioTechniques* **1994**, *17*, 434.
(15) Kresheck, G. C.; Hwang, J. *J. Chem. Phys. Lipids* **1995**, *76*, 193.
(16) Fendler, J. H. *Membrane Mimetic Chemistry*; Wiley: New York, 1982.
(17) Gratzel, M. *Heterogeneous Photochemical Electron Transfer*; CRC Press: Boca Raton, FL, 1989.
(18) Molina-Bolivar, J. A.; Aguiar, J.; Ruiz, C. C. *J. Phys. Chem. B* **2002**, *106*, 870.
(19) Sarkar, N.; Datta, A.; Das, S.; Bhattacharyya, K. *J. Phys. Chem.* **1996**, *100*, 15483.
(20) Sen, P.; Mukherjee, S.; Halder, A.; Bhattacharyya, K. *Chem. Phys. Lett.* **2004**, *385*, 357.
(21) Bhattacharyya, K. *Chem. Commun.* **2008**, 2848.
(22) Bhattacharyya, K.; Bagchi, B. *J. Phys. Chem. A* **2000**, *104*, 10603.
(23) Mondal, S. K.; Sahu, K.; Bhattacharyya, K. *Rev. Fluor.* **2007**, *4*, 157.
(24) Bhattacharyya, K.; Bagchi, B. *J. Phys. Chem. A* **2000**, *104*, 10603.
(25) Nandi, N.; Bhattacharyya, K.; Bagchi, B. *Chem. Rev.* **2000**, *100*, 2013.
(26) Hara, K.; Kuwabara, H.; Kajimoto, O. *J. Phys. Chem. A* **2001**, *105*, 7174.
(27) Kumbhakar, M.; Goel, T.; Mukherjee, T.; Pal, H. *J. Phys. Chem. B* **2005**, *109*, 14168.
(28) Kumbhakar, M.; Nath, S.; Mukherjee, T.; Pal, H. *J. Chem. Phys.* **2004**, *120*, 2824.
(29) (a) Sarkar, N.; Datta, A.; Das, S.; Bhattacharyya, K. *J. Phys. Chem.* **1996**, *100*, 15483. (b) Datta, A.; Mandal, D.; Pal, S. K.; Bhattacharyya, K. *J. Mol. Liq.* **1998**, *77*, 121.
(30) Nandi, N.; Bagchi, B. *J. Phys. Chem. B* **1997**, *101*, 10954.
(31) (a) Pal, S.; Balasubramanian, S.; Bagchi, B. *J. Chem. Phys.* **2002**, *117*, 2852. (b) Pal, S.; Balasubramanian, S.; Bagchi, B. *J. Phys. Chem. B* **2003**, *107*, 5194.
(32) (a) Pal, S.; Balasubramanian, S.; Bagchi, B. *Phys. Rev. E* **2003**, *67*, 061502. (b) Balasubramanian, S.; Pal, S.; Bagchi, B. *Phys. Rev. Lett.* **2002**, *89*, 115505−1.
(33) Hazra, P.; Chakrabarty, D.; Chakraborty, A.; Sarkar, N. *Chem. Phys. Lett.* **2003**, *38*, 271.
(34) Dutt, G. B. *J. Phys. Chem. B* **2003**, *107*, 3131.
(35) Dutt, G. B. *J. Phys. Chem. B* **2002**, *106*, 7398.
(36) Quitevis, E. L.; Marcus, A. H.; Fayer, M. D. *J. Phys. Chem.* **1993**, *97*, 5762.
(37) Maiti, N. C.; Krishna, M. M. G.; Britto, P. J.; Periasamy, N. *J. Phys. Chem. B* **1997**, *101*, 11051.
(38) Maroncelli, M.; Fleming, G. R. *J. Chem. Phys.* **1987**, *86*, 6221.
(39) Fee, R. S.; Maroncelli, M. *Chem. Phys.* **1994**, *183*, 235.
(40) Schott, H.; Royce, A. E.; Hans, S. K. *J. Colloid Interface Sci.* **1984**, *98*, 196.
(41) Maroncelli, M.; MacInnis, J.; Fleming, G. R. *Science* **1989**, *243*, 1674.